

Synthesis of horizontally aligned ZnO nanowires localized at terrace edges and application for high sensitivity gas sensor

J. Y. Son, S. J. Lim, J. H. Cho, W. K. Seong, and Hyungjun Kim

Citation: [Applied Physics Letters](#) **93**, 053109 (2008); doi: 10.1063/1.2967871

View online: <http://dx.doi.org/10.1063/1.2967871>

View Table of Contents: <http://scitation.aip.org/content/aip/journal/apl/93/5?ver=pdfcov>

Published by the [AIP Publishing](#)

Articles you may be interested in

[ZnO nanowires prepared by hydrothermal growth followed by chemical vapor deposition for gas sensors](#)

J. Vac. Sci. Technol. B **27**, 1667 (2009); 10.1116/1.3137020

[Gas sensing properties of defect-controlled ZnO-nanowire gas sensor](#)

Appl. Phys. Lett. **93**, 263103 (2008); 10.1063/1.3046726

[Highly sensitive ZnO nanowire ethanol sensor with Pd adsorption](#)

Appl. Phys. Lett. **91**, 053111 (2007); 10.1063/1.2757605

[ZnO nanowire field-effect transistor and oxygen sensing property](#)

Appl. Phys. Lett. **85**, 5923 (2004); 10.1063/1.1836870

[Fabrication and ethanol sensing characteristics of ZnO nanowire gas sensors](#)

Appl. Phys. Lett. **84**, 3654 (2004); 10.1063/1.1738932

The advertisement features a dark blue background with three images: a mobile phone, a desktop computer, and an AFM. Text on the left asks 'You don't still use this cell phone or this computer' and 'Why are you still using an AFM designed in the 80's?'. Text on the right promotes an upgrade to a modern AFM, offering a \$20,000 trade-in discount and identifying Asylum Research as the technology leader. The Oxford Instruments logo and tagline 'The Business of Science' are at the bottom right, along with the email address dropmyoldAFM@oxinst.com.

Synthesis of horizontally aligned ZnO nanowires localized at terrace edges and application for high sensitivity gas sensor

J. Y. Son,¹ S. J. Lim,¹ J. H. Cho,² W. K. Seong,³ and Hyungjun Kim^{1,a)}

¹Department of Materials Science and Engineering, Pohang University of Science and Technology (POSTECH), Pohang 790-784, Republic of Korea

²RCDAMP and Department of Physics, Pusan National University, Pusan 609-735, Republic of Korea

³Korea Electronics Technology Institute (KETI), Seongnam 463-816, Republic of Korea

(Received 20 May 2008; accepted 14 July 2008; published online 6 August 2008)

We developed step edge decoration method for the fabrication of semiconductor ZnO nanodots and nanowires using pulsed laser deposition. We synthesized high quality ZnO nanowires with the small diameter of about 20 nm and the uniform interval of about 80 nm between each nanowire, which has a simple structure for the formation of contact electrodes. The ZnO nanowire-based sensor was prepared only with the simple process of a gold electrode formation. The ZnO nanowire-based sensor exhibited the high surface-to-volume ratio of $58.6 \mu\text{m}^{-1}$ and the significantly high sensitivity of about 10 even for the low ethanol concentration of 0.2 ppm. © 2008 American Institute of Physics. [DOI: 10.1063/1.2967871]

Recently, “step edge decoration” method emerged as an alternative process producing horizontally oriented nanowires at step edges.^{1–5} The step edge decoration usually produces relatively thicker nanowires with hundreds nanometer diameter (or width) than those produced by other vapor phase based nanowire synthesis methods.^{6,7} In addition, nanowires prepared by step edge decoration are composed of mixtures of nanowires and nanodots, since simultaneous formation of nanodots occurs on terraces besides the formation of nanowires along the step edges and their size distributions are considerably large.^{6,7}

Meanwhile, ethanol sensors have been widely used in biomedical and chemical industries, for the inspection of wine quality, food degradation, and breath analysis.^{8–11} Semiconductor nanowires including SnO_2 , TiO_2 , Fe_2O_3 , and ZnO have been widely studied for general purpose gas sensor applications since nanowire sensors have high sensitivity resulting from their high surface-to-volume ratio.¹² Among various semiconductor nanowires based sensors, ZnO nanowire-based sensors showed relatively high sensitivity for ethanol sensing.^{8,10} In this study, well controlled and localized ZnO nanodots and nanowires were formed at step edges without unnecessary formation of nanodots on terraces. ZnO nanowire sensor was fabricated only with photolithography and high sensitivity was achieved.

ZnO nanodots and nanowires were deposited on (0001) sapphire substrate by eclipse pulsed laser deposition (PLD) method. To prepare uniform terraces on (0001) sapphire substrate, we annealed a miscut sapphire substrate at 1200 °C for 1 h. Commercially available 1 in. ZnO target was used for the laser ablation. A frequency tripled (355 nm) neodymium-doped yttrium aluminum garnet laser was used for the deposition with a target-to-substrate distance of 5 cm and the laser power was approximately 2 J/cm². After the base pressure of $\sim 5 \times 10^{-7}$ Torr was reached, we used optimum deposition conditions of growth temperature of 700 °C and the oxygen partial pressure of 100 mTorr. Gold electrodes were formed by evaporation and they were an-

nealed at 400 °C for 30 min. For the ethanol gas-sensing measurement, ethanol-air mixed gas was introduced into the testing tube at room temperature. The total gas flow rate of about 1 l/min was passed through the quartz tube. For the ZnO nanowire gas sensor, resistance as a function of time was measured in the ethanol concentration ranges of 0.2–200 ppm by a Keithley 4200 system.

Since step edges of terraces are energetically favorable for the nucleation of adatoms, low deposition rate is favorable for producing localized nucleation at step edges of terraces.³ To minimize the ZnO deposition rate, we used low laser pulse repetition rate of 2 Hz and a shadow mask which blocks direct ZnO plume generated by laser ablation. Most ZnO adatoms in the ZnO plume are blocked by the shadow mask and a very small number of ZnO adatoms can immigrate into the substrate surface by scattering with oxygen ambient gas. Thus, oxygen partial pressure directly influences the immigration of ZnO adatoms which affects the ZnO deposition rate. We determined the optimum oxygen partial pressure as 100 mTorr by measuring the ZnO thickness and observing the shape of ZnO plume which distinguishably changes its shape with the variation of oxygen partial pressure. After all, we achieved very low deposition rate of 0.04 Å/pulse, resulting in well localized ZnO nucleation at step edges of terraces.

ZnO nanostructures showed high crystallinity at high growth temperature above 600 °C, which was confirmed by comparisons of full width at half maximum (FWHM) values for x-ray diffraction (002) peak of ZnO nanostructures and thin films. In addition, ZnO nanodots and nanowires exhibited poor uniformity in their sizes for low growth temperature below 600 °C and high growth temperature above 800 °C. Thus, we determined the optimum growth temperature as 700 °C. As the deposition proceeds, ZnO nanostructures change their shapes from nanodots to nanowires, as shown schematically in Fig. 1.

First, we observed morphological features of terraces, nanodots, and nanowires by atomic force microscope (AFM), as shown in Fig. 2. By annealing the substrate at proper conditions, well aligned terraces with the uniform in-

^{a)}Electronic mail: hyungjun@postech.ac.kr.

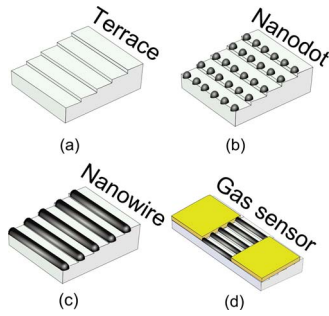


FIG. 1. (Color online) Schematic draws of (a) uniform terraces formed on Al_2O_3 substrate, (b) nanodots grown on terrace, (c) nanowires grown on terrace, and (d) nanowire-based gas sensor on terrace.

terval of about 80 nm between each terrace were formed on (0001) sapphire substrate surface [Fig. 2(a)]. For the ZnO PLD of 120 laser pulses, ZnO nanodots were formed with the diameter of about 5 nm, with the standard deviation in diameter of about 0.8 nm [Fig. 2(b)]. Here, we defined diameter as the FWHM of profile from AFM measurement (shown as insets in Fig. 2). As the number of laser pulses increases, the diameter of nanodots also increased accordingly. For 190 laser pulses, the diameter of ZnO nanodots was about 10 nm with the standard deviation of about 0.6 nm [Fig. 2(c)]. When laser pulses increase above 190 times, nanostructures of a dumbbell shape were observed resulting from coalescence of each nanodots (not shown). After this, these nanostructures became connected to each other to form continuous nanowires. For 340 laser pulses, well aligned ZnO nanowires with the diameter of 20 nm and the thickness of 15 nm were obtained and the standard deviation of the diameter was approximately 1.4 nm [Fig. 2(d)]. All these ZnO nanodots and nanowires with uniform size distribution were well localized only at the edges of terraces.

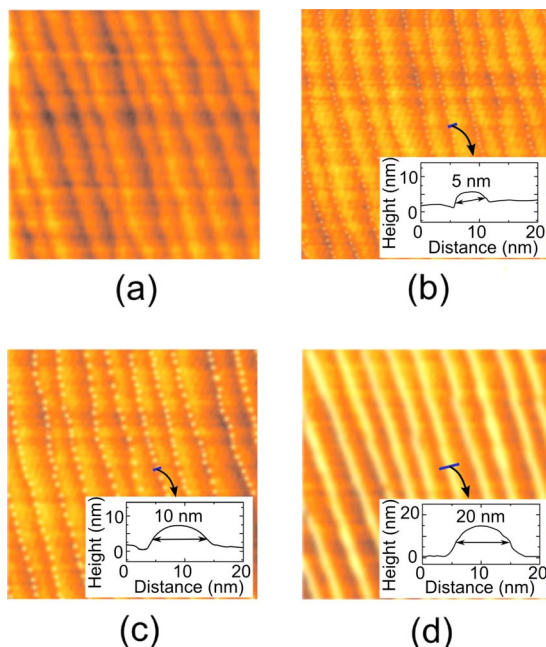


FIG. 2. (Color online) AFM images of (a) terraces formed on Al_2O_3 substrate, (b) nanodots with the diameter of about 5 nm grown on terrace, and (c) nanodots with the diameter of about 10 nm grown on terrace. (d) Nanowires grown with 20 nm diameter on terrace.

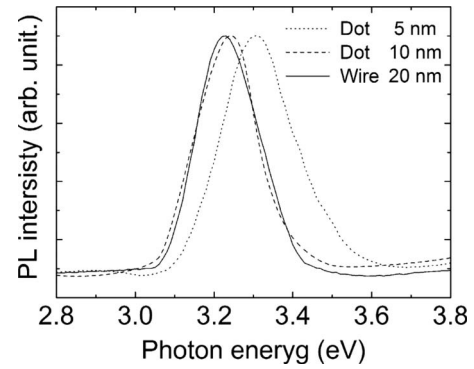


FIG. 3. PL intensities as a function of photon energy for nanodots with the diameter of about 5 nm grown on terrace, nanodots with the diameter of about 10 nm grown on terrace, and nanowires grown with 20 nm diameter on terrace.

We measured photoluminescence (PL) spectra of ZnO nanostructures excited by He–Cd laser (325 nm) at room temperature (Fig. 3). The PL spectrum of ZnO nanowires with the diameter of 20 nm has the PL peak position at 3.22 eV which is similar to the PL peak position of ZnO thin films.¹³ For ZnO nanodots, we observed blueshift in PL peak positions at 3.31 and 3.24 eV for diameters of 5 and 10 nm, respectively. As the size of nanodots decreases, the PL peak position shifts to high photon energy, which is originated from quantum confinement effects of ZnO nanodots.¹⁴ In addition, these PL peaks have low FWHM values below 0.1 eV indicating uniform size distributions.

We fabricated an ethanol gas sensor consisted of these ZnO nanowire array, as shown schematically in Fig. 1(d). The gas sensor consists of 24 nanowires with the exposed length of about $10\ \mu\text{m}$ [Fig. 4(a)]. The surface-to-volume ratio of this ZnO nanowire-based sensor was calculated to be about $58.6\ \mu\text{m}^{-1}$ from the width of 20 nm (the thickness of 15 nm) and the exposed length of about $10\ \mu\text{m}$ for ZnO nanowires. This high surface-to-volume ratio is due to the high aspect ratio of nanowires ($\text{AR} \sim 500$). We measured the current as a function of voltage for the ZnO nanowire gas sensor in air environment, confirming that these ZnO nanowires have no disconnection up to a macroscopic scale about $10\ \mu\text{m}$. Au electrodes showed good Ohmic contact with ZnO nanowires [Fig. 4(b)]. The resistivity of the individual ZnO nanowire in air environment was calculated to be about $0.2\ \Omega\ \text{cm}$ from the resistance of the ZnO nanowire-based sensor.

We obtained sensing characteristics in terms of sensitivity, which is represented by $R_{\text{air}}/R_{\text{gas}}$, where R_{air} is the resistance in atmospheric air and R_{gas} is the resistance in ethanol

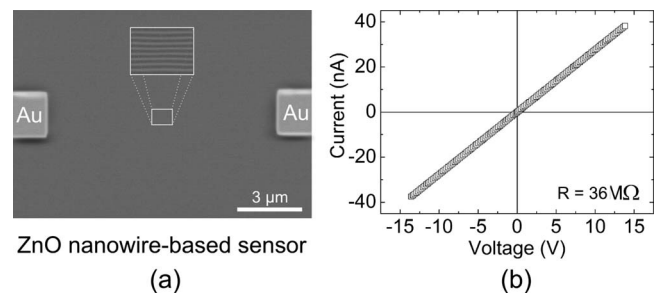


FIG. 4. (a) Scanning electron microscopy image of the ZnO nanowire gas sensor. (b) Voltage dependence of current for ZnO nanowire gas sensor.

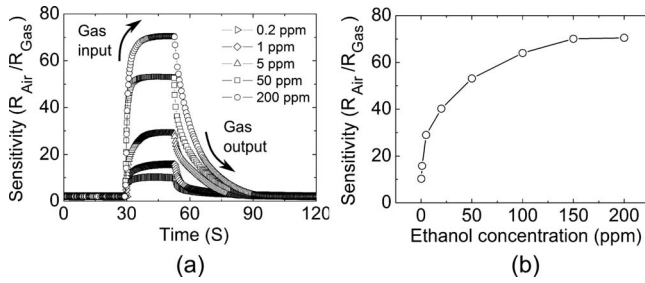


FIG. 5. (a) Response and recovery characteristics of ZnO nanowire gas sensor. (b) Sensitivities as a function of ethanol concentration.

gas environment. As Fig. 5(a) shows, the ZnO nanowire-based sensor well responded to the variation of ethanol concentrations. The ZnO nanowire sensor exhibited good sensitivity ($R_{\text{air}}/R_{\text{gas}}$) of about 10 even for the minimum ethanol concentration of 0.2 ppm. When we increased the ethanol concentration in ethanol-air mixed gas, an increment in sensitivity was clearly observed. The ZnO nanowire sensor showed the sensitivity of about 70 under the condition of the increased ethanol concentration of 150 ppm.

The operating mechanism of ZnO nanowire-based ethanol sensor is similar to other semiconductor gas sensors, which is based on the variation of electrical properties resulting from the adsorption of an analyzed to the surface of sensor materials.¹⁵ Sensitivities as a function of ethanol concentration shows saturation, which indicates that ZnO nanowires become completely conductive surface and even inside of ZnO nanowires over the ethanol concentration of about 150 ppm [Fig. 5(b)]. Consequently, the ZnO nanowire sensor has the significantly high sensitivity especially in a relatively low ethanol concentration region.

The ZnO nanowire sensor fabricated in this study has shown better sensitivity than most of the previous reported ZnO nanowire-based and carbon nanotube-based ethanol sensors [Fig. 5(a)].^{8,10,15-18} For example, Wan *et al.* reported the fabrication of ZnO nanowire sensors with sensitivities of 47 at ethanol concentration of 200 ppm and 1.9 at the ethanol concentration of 1 ppm based on microelectromechanical system technology.¹⁵ We attribute the high sensitivity of the ZnO ethanol sensor fabricated in the current study to the high surface-to-volume ratio, very large length, and high crystallinity of the ZnO nanowires synthesized by PLD. More importantly, it should be noted that a simple device fabrication scheme without using e-beam lithography or dispersion of nanowires was enabled by *in situ* formed horizontal nanowire array synthesized by step edge decoration method.

In summary, we fabricated well arranged ZnO nanodots of 5 and 10 nm diameters and well aligned ZnO nanowires with 20 nm diameter at the edge of terrace steps on the sapphire substrate by the step edge decoration with eclipsed PLD. ZnO nanostructures of nanodots and nanowires were localized at step edges of terraces on sapphire substrate without any deviation from step edges. Quantum confinement effects as size effects were observed in the PL spectra of ZnO nanostructures. The ZnO nanowire-based sensor exhibited the high surface-to-volume ratio of $58.6 \mu\text{m}^{-1}$ and the significantly high sensitivity of about 10 even for the low ethanol concentration of 0.2 ppm.

This work was supported by Korea Research Foundation (Grant Nos. KRF-2007-001-C0111, KRF-2007-331-D00243, KRF-2007-314-C00111, and MOEHRD, KRF-2005-005-J13102), Korea Science and Engineering Foundation (KOSEF) (Grant Nos. R01-2007-000-20143-0 and 2007-02864), Infra Technology Development for Electronic Parts, POSTECH Core Research Program, and Brain Korea 21 Project 2008. J.H.C. was supported by the Korea Research Foundation Grant KRF-2006-005-J02801.

¹M. E. Bourg, W. E. vanderVeer, A. G. Gruell, and R. M. Penner, *Nano Lett.* **7**, 3208 (2007).

²E. J. Menke, Q. Li, and R. M. Penner, *Nano Lett.* **4**, 2009 (2004).

³B. J. Murray, E. C. Walter, and R. M. Penner, *Nano Lett.* **4**, 665 (2004).

⁴M. P. Zach, K. H. Ng, and R. M. Penner, *Science* **290**, 2120 (2000).

⁵B. J. Murray, Q. Li, J. T. Newberg, J. C. Hemminger, and R. M. Penner, *Chem. Mater.* **17**, 6611 (2005).

⁶P. Nguyen, H. T. Ng, T. Yamada, M. K. Smith, J. Li, J. Han, and M. Meyyappan, *Nano Lett.* **4**, 651 (2004).

⁷L. Fernandez, M. Loffler, J. Cordon, and J. E. Ortega, *Appl. Phys. Lett.* **91**, 263106 (2007).

⁸T.-J. Hsueh, C.-L. Hsu, S.-J. Chang, and I. C. Chen, *Sens. Actuators B* **126**, 473 (2007).

⁹J. F. Liu, X. Wang, Q. Peng, and Y. D. Li, *Adv. Mater. (Weinheim, Ger.)* **17**, 764 (2005).

¹⁰H. Ting-Jen, C. Shou-Jinn, H. Cheng-Liang, L. Yan-Ru, and I.-C. Chen, *Appl. Phys. Lett.* **91**, 053111 (2007).

¹¹L. Torsi, M. C. Tanese, N. Cioffi, M. C. Gallazzi, L. Sabbatini, and P. G. Zambonin, *Sens. Actuators B* **98**, 204 (2004).

¹²D. Kohl, *J. Phys. D* **34**, R125 (2001).

¹³C.-W. Lin, D.-J. Ke, Y.-C. Chao, L. Chang, M.-H. Liang, and Y.-T. Ho, *J. Cryst. Growth* **298**, 472 (2007).

¹⁴L. E. Brus, *J. Chem. Phys.* **80**, 4403 (1984).

¹⁵Q. Wan, Q. H. Li, Y. J. Chen, T. H. Wang, X. L. He, J. P. Li, and C. L. Lin, *Appl. Phys. Lett.* **84**, 3654 (2004).

¹⁶L. Liao, H. B. Lu, J. C. Li, C. Liu, D. J. Fu, and Y. L. Liu, *Appl. Phys. Lett.* **91**, 173110 (2007).

¹⁷J. Li, Y. Lu, Q. Ye, M. Cinke, J. Han, and M. Meyyappan, *Nano Lett.* **3**, 929 (2003).

¹⁸Z. Sun, X. Zhang, N. Na, Z. Liu, B. Han, and G. An, *J. Phys. Chem. B* **110**, 13410 (2006).